

# Histological and Biochemical Analysis of The Possible Protective Effects of Luteolin on Testicular Injury Caused by Lead Acetate in Adult Male Albino Rats

Nehal A. Amer<sup>1\*</sup>, Nahla M. Ibrahim<sup>2</sup>, Basma A. Ibrahim<sup>3</sup>, Rasha A. Agaga<sup>1</sup>

## ABSTRACT

### KEYWORDS

Luteolin,  
Lead Acetate,  
Testis Toxicity,  
Rats.

Lead acetate (PbAc) has potential toxic health effects on humans. Information from epidemiological studies proposed that lead environmental exposure may have resulted in reproductive and developmental toxicity. Luteolin is an antioxidant that has antioxidant properties. The study aimed to assess the protective role of luteolin against the toxic effects of PbAc in testis. The study was performed on 40 adult male albino rats divided equally into 4 groups, 10 rats for each group. Group I (Negative control group) was given only a regular diet and tap water. Group II (Luteolin control group) was given Luteolin (50 mg/kg/day) once daily by oral gavage for 4 weeks. Group III (PbAc group) received 50 mg/kg/day in 0.5 ml distilled water by oral gavage for 4 weeks. Group IV (PbAc-Luteolin group) received PbAc and Luteolin with the same doses. After 4 weeks, 24 hours after the last dose, we measured: 1-Total mRNA expressions using RT-PCR of Nrf2, Keap1, NQO1, and HO-1. 2-Testicular oxidative stress markers: MDA, SOD, and GPx activity. 3- Testis Inflammatory cytokines: TNF- $\alpha$  and IL-6. Hematoxylin and Eosin and immunohistochemical examination of the testis were evaluated. In the PbAc-treated rats, there was an elevation in MDA. PbAc caused a decrease in tissue SOD and GPx; TNF- $\alpha$  and IL-6 increased in testis tissues together with elevation of the expression of (Nrf2, Keap1, NQO1, and HO-1). PbAc-induced histological damage and strong immunoreaction for alpha-smooth muscle actin ( $\alpha$ -SMA) and glucose-regulated protein 78 (GRP 78), decreased by co-treatment of luteolin. In conclusion luteolin improved testis function and histology against toxicity of PbAc.

## Introduction

Reproduction is a vital biological feature for producing new individual organisms. Environmental and work-related exposure to toxic elements results in numerous changes to the biological system, and infertility is one of the worldwide public health interests affecting 15% of couples of reproductive ages. The toxic mechanisms are ion imitation, disturbance of cell signaling

pathways, oxidative stress, alteration of gene expression, epigenetic regulation of gene expression, apoptosis, disruption of the testis-blood barrier, inflammation, and endocrine disturbance (Massányi et al., 2020).

Human infertility has resulted in serious problems in societies all over the globe and the male factor accounts for 20%–50% of the infertility patients in humans. Disturbed reproductive function is frequently connected to environmental exposure to toxic materials, including toxic metals, specifically cadmium, lead, and mercury. Lead (Pb) is one of the most frequent heavy metal pollutants upsetting living organisms. This heavy metal occurs naturally in the environment from burning

<sup>(1)</sup> \* Human Anatomy and Embryology Department, Faculty of Medicine, Zagazig University, Egypt

<sup>(2)</sup> Forensic Medicine and Clinical Toxicology Department, Faculty of Medicine, Zagazig University, Egypt,

<sup>(3)</sup> Medical Biochemistry and Molecular Biology Department, Faculty of Medicine, Zagazig University, Egypt. .

fossil fuels, mining, and industry. It also exists in numerous domestic and industrial applications such as the manufacture of ammunition, cosmetics, glass pigments, lead-acid batteries, metal products, oxides for paints, and devices to shield against X-rays. It may exist as a contaminant in diverse sources such as polluted food and water and road traffic (Kelainy et al., 2019; Abdelhamid et al., 2020).

Oxidative stress is one mechanism concerned with testicular toxicity related to lead. Oxidative stress occurs when the creation of reactive oxygen species (ROS) surpasses the capacity of the antioxidant protection system (El-Nekeety et al., 2009). Lead is identified to induce lipid peroxidation of cells and drop in the actions of antioxidant enzymes with excessive production of ROS leading to oxidative stress (Udefa et al., 2020).

Inflammation is about to arise next to oxidative stress in tissues. Lead has been stated to adversely disturb the regulation and function of immunity and raise the systemic response to inflammation (Teerasartipan et al., 2020).

Nuclear factor erythroid 2-related factor 2 (Nrf2), a nuclear transcriptional factor assists as a crucial sensor of cellular oxidative stress. In a basal cytoplasmic condition, without significant cellular stress, Nrf2 is discovered bound to Kelch-like ECH-associated protein 1 (Keap1). When ROS overproduction defeats the endogenous antioxidant supplies, Nrf2 is phosphorylated by protein kinase B, released via Keap1, and is translocated in the nucleus and this results in stimulating and transcribing essential cell-protective and antioxidants (Somade et al., 2022; Ulasov et al., 2022).

NAD(P)H dehydrogenase [quinone] 1 (NQO1) and Heme oxygenase 1 (HO-1) are

two genes controlled by Nrf2. Simply, Nrf2 activation is crucial for NQO1 and HO-1 transcription (Li et al., 2014), both are induced genes with antioxidant properties. NQO1 is an antioxidant that catalyzes the reduction in 2-electron quinone to create hydroquinones. In contrast HO-1 catalyzes the conversion of heme to biliverdin, which is then converted to bilirubin by biliverdin reductase, a molecule with antioxidant properties (Ross & Siegel, 2017).

A new strategy has been accepted all over the world which involves the use of natural substances that have a wide range of health-improving capabilities including antioxidant and anti-inflammatory activities might offer a defending effect against the harm made by heavy metals. Flavonoids are well-thought-out therapeutic compounds due to their potent pharmacological properties; hence, they are widely used in medicines and food supplements (Ijaz et al., 2023).

Luteolin (3',4',5,7-tetra-hydroxy-flavone, LUT) is a natural dietary flavonoid that frequently exists in various medicinal plants, vegetables, and fruits like flowers of *Sophora viciifolia*, *Paeonia moutan*, and *Rumex nervosus*, broccoli, celery, pepper, perilla leaf, honeysuckle bloom, and chamomile tea (Albarakati et al., 2020; Ijaz et al., 2022).

Several reports have highlighted the myriad biological effects of luteolin, such as antioxidant, anti-inflammatory, anti-angiogenic, anti-virus replication, anti-diabetic, immunomodulatory, cytoprotective, and anti-apoptotic activities. Furthermore, LUT can cross the blood-brain barrier and act as a neuroprotective agent. Moreover, Kempuraj et al. (2021) stated that LUT suppresses systemic and neuro-inflammatory responses in coronavirus disease 2019 (COVID-19) (Ijaz et al., 2022).

New researches have revealed the advantageous properties of LUT in diverse experimental models. LUT-induced renal tissue protection against nephrotoxicity by preventing oxidative damage, inflammation, and activation of antioxidant signals in rats (Baty et al., 2020).

Additionally, LUT improved the lung injury occurring due to cadmium exposure and induced an activation of the antioxidant defense system (Owumi et al., 2020).

There was a need to carry out a scientific investigation on the male sexual parameters of the protective and ameliorative capacities of the luteolin to corroborate the ethnomedical use of the luteolin as an antioxidant against other male reproductive dysfunctions. Therefore, we seek, in this study, to assess the effects of luteolin on lead acetate-damaged testes of adult male albino rats.

## Materials and Methods:

### Chemicals

We purchased 99 percent Pb acetate from Piochem Company. The source of luteolin (CAS number 855-97-0) was Alfa Aesar in Kandel, Germany. All the chemicals and reagents were brought in the analytical grade. In this investigation, double-distilled water served as the solvent. We took in distilled water from Kemecta Company.

### Animals

Forty healthy adult male albino (Sprague Dawley) rats, weighing 200–250 g, were used in the study. They came from the animal house of Zagazig University's Faculty of Medicine. The animals had been housed in clean, well-ventilated polypropylene cages with stainless steel covers, wood shaving bedding, regular supplies, and flowing water.

They were maintained at  $23\pm 2$  degrees Celsius. The rats spent two weeks adapting to the lab environment before starting the experiment. The experiment's rats were handled in agreement with the Zagazig University Institutional Animal Care and Use Committee's (ZU-IACUC) typical operating procedures and approval number (ZU-IACUC/3/F/245/2023) and was carried out following ARRIVE guidelines.

### Experimental protocol

Four primary groups of rats (10 for each) were randomly assigned, and the rats received oral gavage treatment for four weeks to administer the drugs.

**Group I:** Control group (10 rats): (negative control with no treatment all through the experiment to measure basal parameters.

**Group II:** Luteolin (LUT) group (10 rats): which will receive Luteolin 50 mg/kg once per day by oral gavage for 4 weeks.

**Group III:** Lead Acetate (PbAc) treated group (10 rats): which will receive 50 mg/kg/day in 0.5 ml distilled water, oral gavage for 4 weeks (Hamdan et al., 2020).

**Group IV:** Lead Acetate-Luteolin (PbAc+LUT) treated group (10 rats): which will receive 50 mg/kg/day of PbAc in 0.5 ml distilled water, oral gavage for 4 weeks, and 50 mg/kg luteolin once per day by oral gavage for 4 weeks (Kalbolandi et al., 2019).

### Biochemical Assays

#### *Testicular Oxidative Stress Parameters Analysis*

The rats were humanly executed, and their testes were removed and prepared for further study. One testis from each rat was preserved in formalin for examination under a

microscope, while the other was used to create a mixture of cells for biochemical and molecular analysis. Following the manufacturer's guidelines, the level of Malondialdehyde (MDA), testicular oxidative stress indicator was assessed following the thiobarbituric acid manner of Ohkawa et al. (1979) using a bio-diagnostic kit (Cat. No. MD 2529, Giza, Egypt), superoxide dismutase (SOD) and glutathione peroxidase (GPx), antioxidant enzymes that were assayed following the method of Marklund and Marklund (1974) and Paglia and Valentine (1967) using commercial bio-diagnostic kits (Cat. No. SD 2521, bio-diagnostic.com, Giza, Egypt) for SOD and (Cat. No. GP 2524, Giza, Egypt) for GPx.

#### **Determination of Inflammatory Cytokines**

The whole blood was obtained from each rat and placed in plain tubes for biochemical analysis. After 30 min at room temperature, the blood was centrifuged for 5 min at 10,000 rpm and 4°C to obtain serum. By the manufacturer's instructions, sera were employed to quantify IL-6 and TNF- $\alpha$  using a readily available rat ELISA kit; (IL-6 (Rat) ELISA Kit, Cat. No. K4145-100, BioVision, Milpitas, USA), and (TNF- $\alpha$  (Rat) ELISA Kit, Cat. No. K1052-100, BioVision,

Milpitas, USA), and results were normalized to the standard curves.

#### **Gene Expression Analysis**

The rats' testicular tissues were homogenized, and total RNA was extracted using Trizol<sup>TM</sup> reagent orders (Invitrogen; Thermo Fisher Scientific, USA). Complementary DNA (cDNA) was generated via HiSenScript<sup>TM</sup> RH (-) cDNA Synthesis Kit (iNtRON, Biotechnology, USA). Quantitative real-time PCR was performed in Mx3005P real-time PCR system (Agilent Stratagene, USA): 10  $\mu$ L TOPreal<sup>TM</sup> qPCR 2X PreMIX (SYBR Green with low ROX) (Cat. # RT500S or RT500M) (Enzymomics, Korea), 1  $\mu$ L of each primer, 3  $\mu$ L cDNA, and 5  $\mu$ L RNAase-free water in 20  $\mu$ L final volume. The qPCR thermal cycling program includes initial denaturation at 95°C for 12 min, then 40 cycles of 95°C for 20 s, 60°C for 30 s, and 72°C for 30 s. Relative mRNA genes Nrf2, Keap1, NQO1, and HO-1 were normalized to  $\beta$ -actin expression. Relative expression values were calculated as fold-changes using the  $2^{-\Delta\Delta CT}$  method (Livak and Schmittgen, 2001), primers sequence (synthesized by Invitrogen, Thermo Fisher Scientific) listed in table (1).

**Table (1):** Primers Sequences.

Genes	Primers (5' to 3')	Accession number	Product length (bp)
<b>Nrf2</b>	F: CAGCATGATGGACTTGGAATTG R: GCAAGCGACTCATGGTCATC	NM_031789.3	414
<b>Keap1</b>	F: TGAAGTGACCCGCTTGACAT R: CCCAGGAGAAGTGTCACAGAA	NM_057152.2	893
<b>NQO1</b>	F: AGCGCTTGACACTACGATCC R: TCTGCGTGGGCCAATACAAT	NM_017000.3	80
<b>HO-1</b>	F: GGCTTTAAGCTGGTGATGGC R: GGGTTCTGCTTGTTTCGCTC	NM_012580.2	80
<b><math>\beta</math>-actin</b>	F: GATTACTGCTCTGGCTCCTAGC R: GACTCATCGTACTCCTGCTTGC	NM_031144.3	147

***Histopathological examination for testis:***

Testis tissue samples were put in a 10% neutral buffered formalin solution for histopathology. were then ready for immersion in paraffin wax, slices were cut to a thickness of 5um, and Mallory trichrome and hematoxylin and eosin (H&E) staining were applied (Bancroft and Gamble, 2008). Each animal's five unique, non-overlapping sections were examined under a light microscope at the anatomy department of Zagazig University, where they were also photographed.

***Immunohistochemical examination.***

Serial sections that had been sliced were put on coverings made of poly-lysine. After boiling for ten to twenty minutes in 10 mM citrate buffers (PH 6.0), tissue slices were allowed to cool for twenty minutes at room temperature. Two rounds of slide washing were conducted using phosphate-buffer saline (PBS). The following primary antibodies (1ry Ab) were used:

***Immunohistochemical staining for detecting alpha-smooth muscle actin ( $\alpha$ -SMA):***

Monoclonal mouse anti-human  $\alpha$ -SMA (N 1584, Dako, Carpinteria, California, USA) was utilized as the primary antibody. The immune expression of  $\alpha$ -SMA manifested as brown staining of the cytoplasm.

***Immunohistochemical staining for detecting Glucose-regulated protein 78 (GRP78):***

The testicular tissues were submerged in Bouin's solution and then embedded in paraffin. After that, five-micrometer sections were rehydrated in alcohol after being deparaffinized in toluene. The anti-glucose regulated protein 78 (anti-GRP78) antibody (sc-1501, Santa Cruz Biotechnology, California, USA) was diluted at 1:50 and left

for the entire night at 4 °C. The sections were incubated with peroxidase-conjugated anti-goat IgG secondary antibody (ZhongShan Biotechnology Co, Beijing, China) for one hour at room temperature following three washes in PBS-T (phosphate-buffered saline (PBS) containing 0.05% (v/v) Tween 20). By employing a DAB kit, peroxidase activity was discovered (ZhongShan Biotechnology). Instead of utilizing polyclonal antibodies against GRP78, the same concentration of commercial goat IgG was used as a negative control. Sections were then mounted in a water-based media and counterstained with Harris's hematoxylin containing glycerol and Mowiol (Calbiochem; EMD Biosciences Inc, La Jolla, California, USA) as preservatives (Wang et al., 2014).

***Image Analysis***

For each rat in each group, 10 fields from 5 sections were coded for blind inspection and assessment. ImageJ software (ImageJ/Fiji 1.46r, <https://imagej.nih.gov/ij/index.html>) was used to examine the assessment of images. From each H&E-stained section, five fields were selected at random and photographed at a 400x objective lens magnification. The perimeter of seminiferous tubules and their epithelial height were analyzed using the National Institutes of Health's Image-J program (version 1.51k, Wayne Rasband, USA) (Melebar, 2022).

***Statistical Analysis***

The data obtained from the experimental rats were expressed as mean  $\pm$  standard deviation (SD) and analyzed statistically using one-way analysis of variance (ANOVA) followed by Tukey's multiple comparisons post hoc test on GraphPad Prism 8.0 statistical software package. Results were considered significant

when  $p$ -value was  $<0.05$  and statistically highly significant difference when  $p<0.0001$ .

## Results

### Biochemical Results of Oxidative Stress Parameters and Inflammatory Cytokines

Regarding the oxidative parameters, rats exposed to PbAc had a statistically significantly higher level of MDA than the control group ( $p<0.0001$ ) suggesting testicular oxidative damage. While in the

PbAc +LUT-treated class, there was a statistically significantly diminution compared to the PbAc-exposed class ( $p<0.0001$ ) indicating decreased lipid peroxidation. Conversely, there was a statistically noteworthy decline of the antioxidant enzymes, SOD and GPx in PbAc-exposed rats compared to the controller ( $p<0.0001$ ). While in the PbAc+LUT-treated class, there was a statistically noteworthy increase compared with the PbAc-exposed class ( $p<0.0001$ ) (Figure 1. A&B&C).

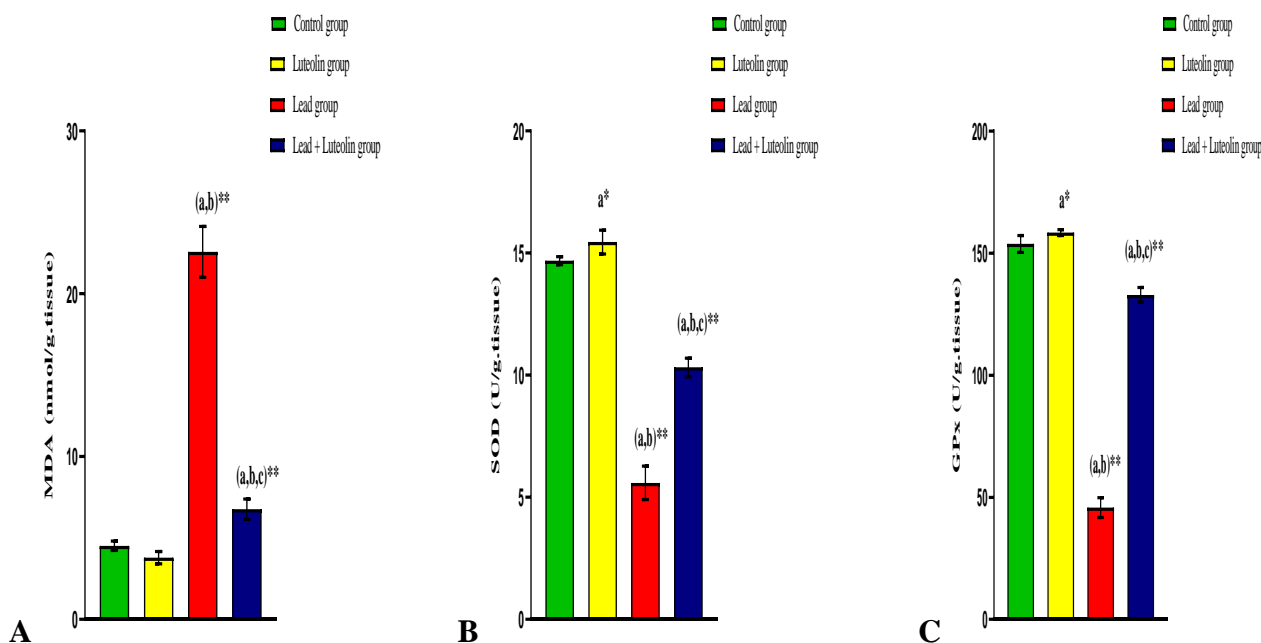


**Fig. (1):** The effect of lead exposure and luteolin treatment on testicular oxidative stress markers in male rats. **(A)** Testicular MDA level (nmol/g.tissue), **(B)** testicular SOD level (U/g.tissue), and **(C)** testicular GPx level (U/g.tissue). The data expressed as mean $\pm$ SD, \*statistically significant difference ( $p<0.05$ ), \*\*statistically highly significant difference ( $p<0.0001$ ), <sup>a</sup> significant when compared to the control group, <sup>b</sup> significant when compared to the luteolin group, and <sup>c</sup> significant when compared to the lead group.

There was a statistically meaningful enhancement in the quantities of IL-6 and TNF- $\alpha$  in PbAc-exposed rats compared to the

controller ( $p<0.0001$ ) which became reversed in the PbAc+LUT-treated class compared to the PbAc-exposed class ( $p<0.0001$ ) (Table 2).

**Table (2):** Inflammatory markers among different experimental groups.

	Group I (Control group) n=10	Group II (Luteolin group) n=10	Group III (Lead group) n=10	Group IV (Lead+Luteolin group) n=10	p-value
<b>IL-6</b> (pg/mL)	19.97±0.35	19.36±0.25	65.58±2.28 <sup>a,b**</sup>	42.65±2.51 <sup>a,b,c**</sup>	<0.0001**
<b>TNF-α</b> (pg/mL)	31.57±2.21	30.03±0.75	90.16±1.77 <sup>a,b**</sup>	56.44±4.68 <sup>a,b,c**</sup>	<0.0001**

n: number, \*\*Statistically highly significant difference ( $p < 0.0001$ ), <sup>a</sup> Significant when compared to the control group, <sup>b</sup> Significant when compared to the luteolin group, and <sup>c</sup> Significant when compared to the lead group.

### The Real-Time Quantitative PCR

The entire testicular mRNA expression of Nrf2 was significantly heightened when PbAc was administered compared with control (1.99±0.26, 0.89±0.08-fold-change respectively ( $p < 0.0001$ )). Following LUT treatment there was a significant reduction in the Nrf2 level compared with PbAc only (1.09±0.08, 1.99±0.26-fold-change respectively ( $p < 0.0001$ )). Also, the Keap1 testicular mRNA expression was considerably raised after PbAc exposure compared with the control (1.67±0.07, 1.03±0.12-fold-change respectively ( $p < 0.0001$ )). LUT treatment significantly lessened ( $p < 0.0001$ ) the testicular Keap1 amount, compared with

PbAc only (1.04±0.13, 1.67±0.07-fold-change respectively ( $p < 0.0001$ )) (Figure 2).

The testicular NQO1 mRNA level was significantly increased in PbAc-exposed rats judged with controller (2.45±0.32, 0.94±0.13-fold-change respectively ( $p < 0.0001$ )). LUT treatment significantly decreased the NQO1 level compared with PbAc only (1.70±0.10, 2.45±0.32-fold-change respectively ( $p < 0.0001$ )). Similarly, HO-1 mRNA expression in the testis was significantly increased following PbAc exposure compared with control (2.03±0.23, 0.97±0.12-fold-change respectively ( $p < 0.0001$ )). Treatments with LUT significantly reduced the HO-1 mRNA level compared with PbAc only (1.21±0.07, 2.03±0.23-fold-change respectively ( $p < 0.0001$ )) (Figure 2).

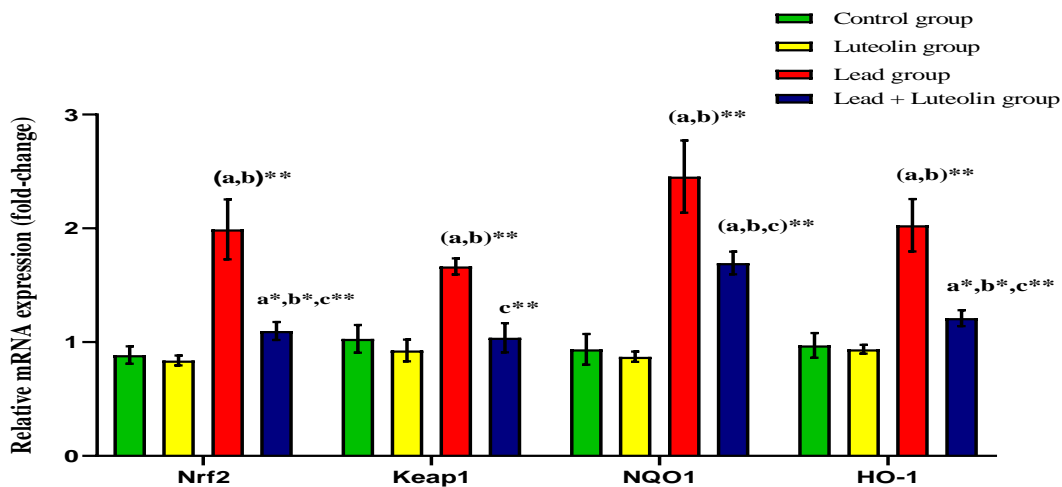
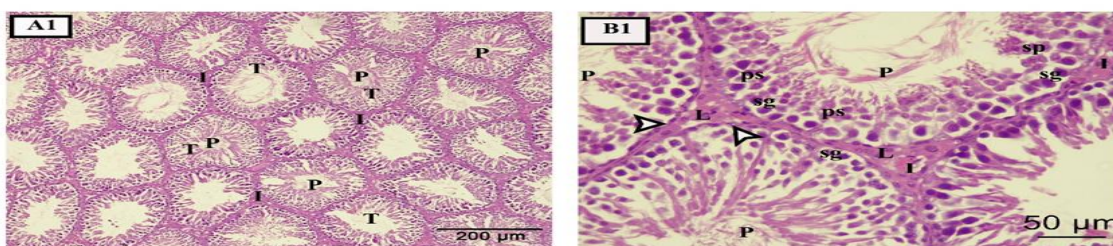


**Fig. (2):** Testis total mRNA relative expression of Nrf2, Keap1, NQO1, and HO-1 in the different experimental groups. \*Statistically significant difference ( $p < 0.05$ ), \*\*statistically highly significant difference ( $p < 0.0001$ ), <sup>a</sup> significant when compared to the control group, <sup>b</sup> significant when compared to the luteolin group, and <sup>c</sup> significant when compared to the lead group.

**Hematoxylin and Eosin Staining Results:**

The testicular parenchyma of control adult albino rats' testes, when examined under a light microscope and stained with H&E, showed that the seminiferous tubules were closely packed. A regular basement membrane supported a well-organized, stratified germinal epithelium lining the tubules. In the lumina of certain tubules, sperm were visible. There was a small space

between them that had Leydig cell clusters in it. Different kinds of spermatogenic cells were visible in the stratified germinal epithelium. Small, spherical cells with rounded nuclei were known as spermatogonia. Spherical nuclei grouped in one or two layers gave the appearance of being giant primary spermatocytes. Spermatids had pale nuclei. Spermatozoa were observed in the tubule lumina (Figure 3. A1 & B1).

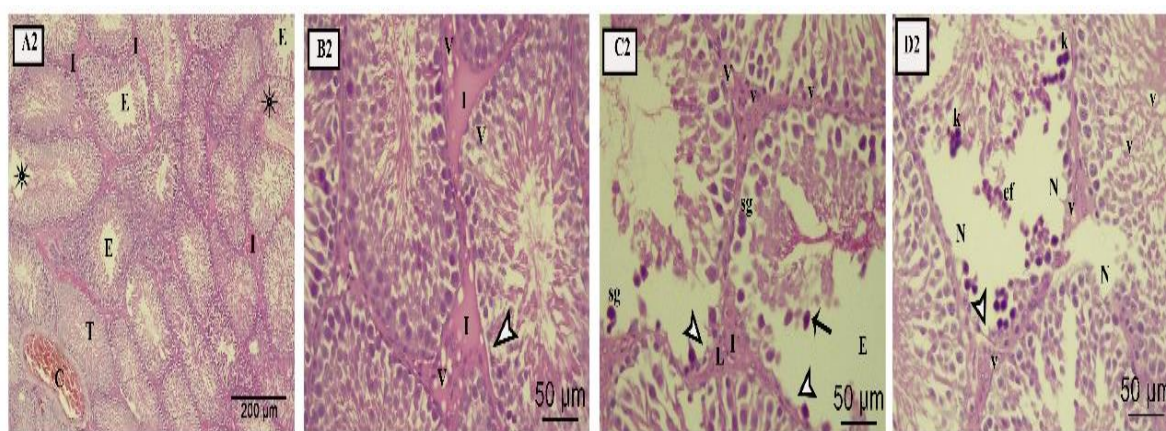


**CONTROL GROUP**

**Fig. (3):** A photomicrograph of the control group's rat testis tissue stained with H&E. **A1:** Demonstrates the testicular parenchyma, which is made up of densely clustered seminiferous tubules (T) and sperm aggregations (P) visible in the lumina. Cell clusters can be seen in the small interstitial spaces (I). [Scale bar X200, H&E X100]. **B1:** An enlarged view of the preceding figure demonstrates densely clustered seminiferous tubules on top of a typical basement membrane (arrowhead). Distinct spermatogenic cells, including spermatids (Sp), spermatogonia (Sg), primary spermatocytes (Ps), and sperms (P). Leydig cells (L) were visible in interstitial space (I). [Scale bar X50, H&E X400].

Testes sections from adult albino rats treated with lead revealed reduced size of the tubules with varying forms and uneven outlines when stained with H&E. Large areas of necrosis, clogged blood arteries, and acidophilic exudates were found in the wide interstitial spaces between tubules (Figure 4. A2 & B2). Deformed seminiferous tubule with many vacuoles separating the haphazard germinal epithelial nuclei highlighted darkly

were found. Sperm-free empty tubules were visible in the lumen. Some exudates were acidophilic in the interstitial space. The nuclei of spermatogonia were disfigured and stained darkly. Within the lumen of a seminiferous tubule, exfoliated cells were visible. There were apoptotic cells present with nuclei stained darkly. One can observe an uneven basement membrane (Figure 4. C2 & A2).



#### TREATED GROUP

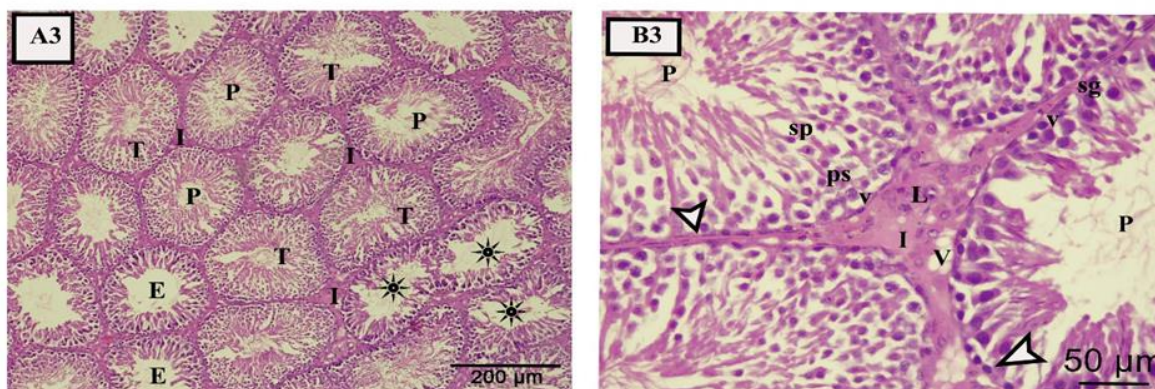
**Fig. (4):** A photomicrograph of the (PbAc) treated group's rat testis tissue stained with H&E. **A2:** demonstrates many reduced tubules (T) with irregular borders. Distorted tubules with irregular shapes and architecture (asterixis), congested blood vessels (c), and pink-colored acidophilic exudates. No sperms were seen in the lumen of empty tubules (E) [Scale bar X200, H&E X100]. **B2:** Demonstrates a deformed seminiferous tubule with many vacuoles (v) sitting between destroyed germinal epithelium (arrowhead) with darkly pigmented nuclei. The acidophilic exudates were found in the interstitial space (I). **C2:** Demonstrates a deformed seminiferous tubule with a partially empty lumen (E), an unorganized germinal epithelium (arrowhead), some exfoliated pyknotic germinal cells (arrow) and malformed spermatogonia (sg) with darkly stained nuclei. Leydig cells (L) were visible in the interstitial space (I) which also contained vacuolated exudate (V). **D2:** Demonstrates a seminiferous tubule's lumen was home to exfoliated cells (ef). There were apoptotic cells (k) with nuclei that were darkly stained. Vacuolated (v) exudate and an uneven basement membrane (arrowhead) were visible. Necrosis (N) and wide gaps between tubules were also noted. [H&E X400, Scale bar X50].

In rats given PbAc+LUT, their testes showed that certain seminiferous tubules had returned to their typical overall structure.

Their spermatogonia and germinal epithelium were positioned normally. The narrow interstitium separated the tubules with

primary spermatocytes, spermatids, and sperms in their lumina. On the other hand, the contours of certain tubules were uneven and deformed. There were several tubules bordered with intact epithelium. In most

tubules, intercellular gaps were seen within the germinal epithelium. In most tubules, the sperm was visible. In the interstitial space, few vacuoles were seen (Figure 5. A3 & B3).



### PROTECTED GROUP

**Fig. (5):** A photomicrograph of the (PbAc+ LUT) treated group's rat testis tissue stained with H&E. **A3:** Demonstrates the return of certain seminiferous tubules (T) to their typical overall morphology. The sperm (p) and germinal epithelium (E) in their lumina were positioned correctly, and small interstitial spaces (I) were visible. Nevertheless, certain tubules exhibited irregular shapes and architecture (asterixis) and empty lumens (E). [H&E X100, Scale bar X200]. **B3:** Demonstrates seminiferous tubules with a typical overall morphology were demonstrated in B3. They had primary spermatocytes (ps), spermatids (sp), well organized germinal epithelium (arrowhead), normal spermatogonia (sg), and sperms (p) in their lumina. The narrow interstitium (I) between them was filled with Leydig cells (L) and some vacuolated exudate (V). [H&E X400, Scale bar X50].

#### *Mallory trichrome staining results:*

Sections of the treated group had an abundance of collagen fibers around congested blood vessels and in the capsule (Figure 6. A2&B2), while sections of the testis of the control group showed few

collagen fibers in the interstitial spaces of the testis around blood vessels (Figure 6. A1 & B1). Some collagen fibers were observed in the testis' interstitial spaces and capsule by the lead + luteolin group (Figure 6. A3 & B3).

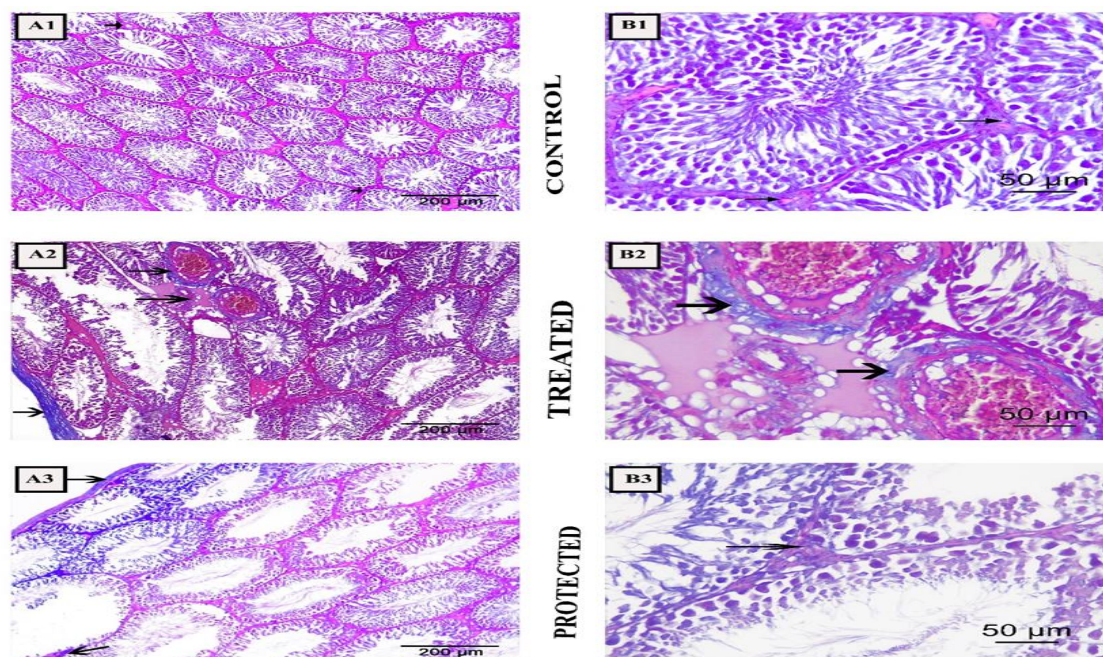


**Fig. (6):** A photomicrograph of the different group's rat testis tissue stained with Mallory trichrome stain; control (A1&B1), PbAc treated (A2&B2) and PbAc+LUT (A3&B3). **A1, B1:** Demonstrate minimal collagen fibers (**arrows**) in the interstitial spaces of the testis and lining of the tubules. **A2, B2:** Demonstrate excess collagen fibers around congested blood vessels and in the capsule (**arrows**). **A3, B3:** Demonstrate some collagen fibers in the interstitial spaces of the testis and the capsule (**arrows**). [Mallory trichrome X100, scale bar 200 and X400, scale bar 50]

#### **Results of immunohistochemical staining for alpha-smooth muscle actin ( $\alpha$ -SMA):**

Alpha-smooth muscle actin ( $\alpha$ -SMA) immunohistochemical localization in the control group demonstrated a mild positive immune reaction (Figure 7. A). Strong

positive immune reaction was observed at the peritubular muscle coat and blood vessel in the lead treatment group (Figure 7. B). The protected group demonstrated moderately positive immune reaction (Figure 7. C).

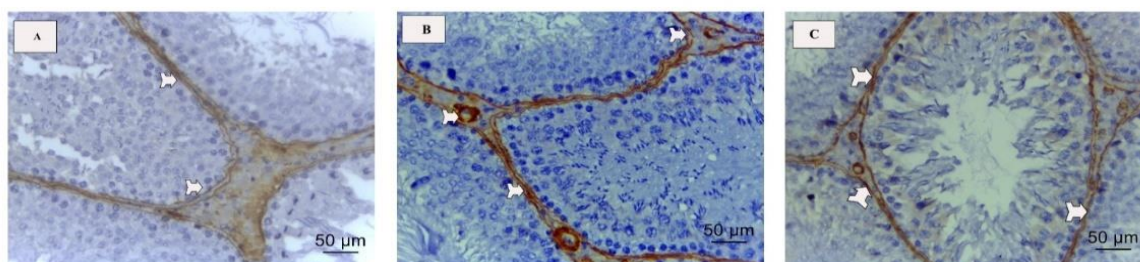


**Fig. (7):** A photomicrograph of the different groups' rat testis tissue stained with  $\alpha$ -SMA immunohistochemical stain, control (A), PbAc treated (B), and PbAc+LUT (C). **A:** Demonstrates mild positive  $\alpha$ -SMA immunohistochemical reaction (**tailed arrow**). **B:** Demonstrates Strong positive  $\alpha$ -SMA immunohistochemical reactions at the peritubular muscular coat and blood vessel (**tailed arrow**). **C:** Demonstrates moderate positive  $\alpha$ -SMA immunohistochemical reaction (**tailed arrow**) [IHC X 400, scale bar 50].

**Glucose-regulated protein 78 (GRP78) immunohistochemical staining results:**

The control group showed negative expression of glucose-regulated protein 78 (GRP78) (Figure 8. A1&B1). The testis of the

lead-treated group showed strong positive cytoplasmic staining (Figure 8. A2 & B2). The lead-luteolin group showed mild positive cytoplasmic staining (Figure 8. A3 & B3).

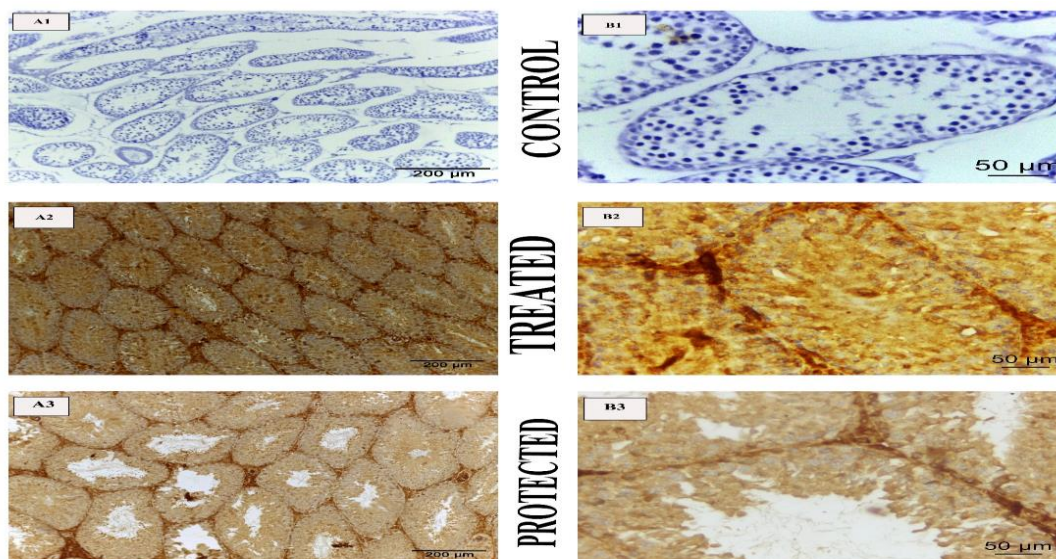


**Fig. (8):** A photomicrograph of the different group’s rat testis tissue stained with glucose-regulated protein78 (GRP78) immunohistochemical stain, control (A1&B1), PbAc treated (A2&B2) and PbAc+LUT (A3&B3). **A1&B1:** Demonstrate negative expression of GRP78. **A2&B2:** Demonstrate strong positive cytoplasmic staining of GRP78. **A3&B3:** Demonstrate mild positive cytoplasmic staining of GRP78. (IHC X100, scale bar 200 and X400, scale bar 50].

**Morphometric results:**

By morphometric analysis, there is a highly significant difference in the perimeter of seminiferous tubules and their epithelial

height in the PbAc-treated group as compared to the control and PbAc+LUT-treated groups (Table 3) and (Figures 9 &10).

**Table (3):** The perimeter and height of seminiferous tubules (ST).

Parameter	Group I (Control group) n=10	Group II (Luteolin group) n=10	Group III (Lead group) n=10	Group IV (Lead+Luteolin group) n=10	p-value
Perimeter of ST (µm)	612±34	612±34	490±31 <sup>a,b**</sup>	604±26 <sup>c**</sup>	<0.0001**
Epithelial height of ST (µm)	39.9±5.8	39.9±5.8	23.3±4.4 <sup>a,b**</sup>	38.8±7.2 <sup>c**</sup>	<0.0001**

The data expressed as mean ± SD, p-value for One-way ANOVA followed by Tukey's multiple comparisons post hoc test, n: number, \*statistically significant difference (p<0.05), \*\*statistically highly significant difference (p<0.0001), <sup>a</sup> significant when compared to the control group, <sup>b</sup> significant when compared to the luteolin group, and <sup>c</sup> significant when compared to the lead group.

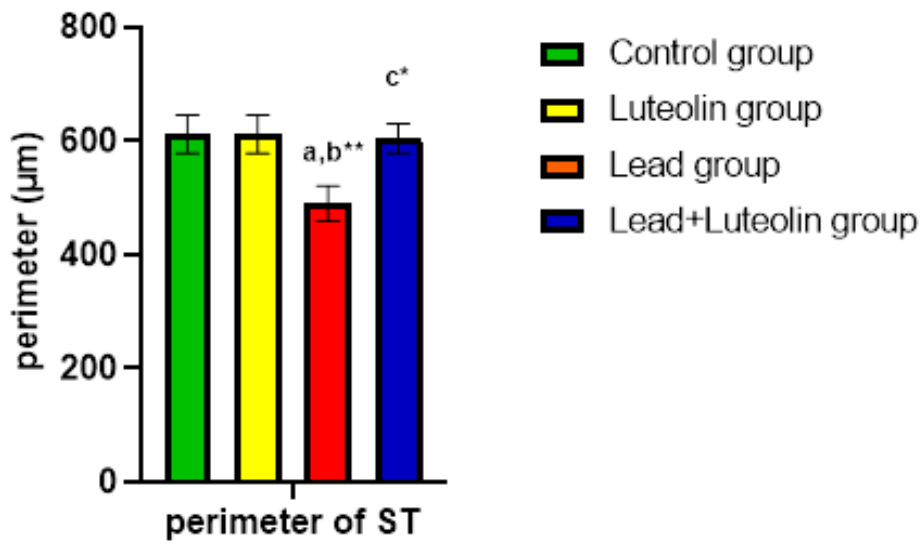


Fig. (9): The perimeter of seminiferous tubules in different studied groups.

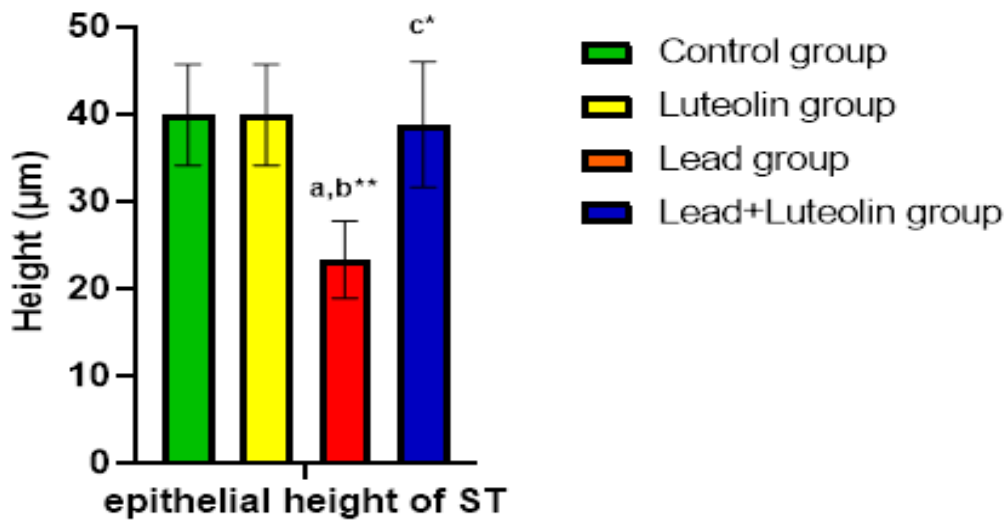


Fig. (10): The epithelial height of seminiferous tubules in different studied groups.

## Discussion:

Industry increases the risk to human life, particularly the male reproductive system, by causing heavy metals to accumulate in the environment and deposit in bodily tissues (Anyanwu et al., 2018).

Lead Acetate (PbAc) is a famous toxin for the reproductive system of the male that increases the generation of free radicals and disrupts sperm synthesis, steroidogenesis, and the normal axis of the hypothalamus-pituitary-testes (Wahab et al., 2019).

According to reports, heavy metals can damage reproductive tissue, which lowers PbAc excretion and increases PbAc buildup in tissues (Elmallah et al., 2017). PbAc can enter the seminiferous tubules because of this disruption of the blood-testis barrier, which is kept in place by the tight connections of Sertoli cells (Mabrouk and Ben Cheikh, 2016).

The valuable explanation of combining luteolin with lead exposure lies in its potential to mitigate the adverse effects of lead toxicity. Studies have demonstrated that luteolin can significantly reduce lead-induced oxidative stress, inflammation, and apoptosis (cell death) in various tissues, including the brain, liver, and kidneys (Rakoczy et al., 2023). Moreover, luteolin has been shown to enhance the body's natural detoxification mechanisms, enhancing the excretion of lead from the body. This proposes that luteolin may be a valuable adjunct therapy for individuals exposed to lead, particularly in occupational or environmental settings (Taheri et al., 2021).

In line with earlier studies (Abdel Moniem, 2012; Elgawish and Abdelrazek, 2014; Sudjarwo et al., 2017), our finding revealed that the exposure of the rats to lead gave rise to a significantly elevated testicular

MDA (lipid peroxidation product) level along with significant decrease in the activities of testicular enzymatic antioxidants SOD and GPx ( $p < 0.0001$ ), suggesting the occurrence of oxidative stress in the testis.

Luteolin administration alone caused a non-significant decrease in MDA level but caused a significant elevation in the antioxidant enzymes SOD and GPx activities ( $p < 0.05$ ), implying its capability to advance the antioxidant defense cascade. Remarkably, luteolin significantly downregulated the MDA level and upregulated the antioxidant enzyme activities in PbAc+LUT treated rats in comparison with PbAc alone ( $p < 0.0001$ ), demonstrating the luteolin ability to fight the oxidative damage caused by PbAc exposure.

To determine the likelihood of inflammation following PbAc exposure, we evaluated the serum concentrations of inflammatory cytokines IL-6 and TNF- $\alpha$ . Our findings revealed that PbAc increased inflammation as the levels of IL-6 and TNF- $\alpha$  were substantially increased in PbAc-exposed rats compared with control ( $p < 0.0001$ ). Conversely, following luteolin treatment, both inflammatory cytokines decreased significantly in PbAc+LUT-treated rats in contrast to PbAc-exposed alone ( $p < 0.0001$ ). These findings suggest that luteolin has an anti-inflammatory impact on PbAc-related inflammation which comes in harmony with the findings of Dyatlov and Lawrence (2002) and Aprioku (2013), who found that the lead was informed to significantly increase serum IL-6 and TNF- $\alpha$  levels in mice.

Our results showed a significant increase in Nrf2 and Keap1 total mRNA expression in PbAc-exposed rats ( $p < 0.0001$ ) which may be an adaptive response to PbAc-induced oxidative stress. The significant drop in antioxidant parameters might indicate ROS excessive production and depletion of endogenous antioxidants, which would have

resulted in cytoplasmic Nrf2 activation and dissociation from Keap1, as well as the reason for their significant rise. The significant decrease in Nrf2 and Keap1 testicular mRNA expressions in LUT-treated rats ( $p < 0.0001$ ) may be attributed to its antioxidant properties that have assisted in the removal of ROS persuaded by PbAc, hence preserving the intrinsic antioxidants, and keeping Nrf2 in its repressive condition (bound to Keap1) in the cytoplasm.

Like Nrf2, we also found a significant elevation in NQO1 and HO-1 testicular mRNA expressions in PbAc-exposed rats ( $p < 0.0001$ ). We assign this to the stimulated and increased Nrf2 expression. The triggered Nrf2 may have translocated to the nucleus and bound to AREs, resulting in the nuclear transcription of NQO1 and HO-1 as well as testicular upregulation of them. Our findings on Nrf2, Keap1, NQO1, and HO-1 concur with those of Li et al. (2014), who showed that polychlorinated biphenyl quinone activated Nrf2/Keap1 and induced NQO1 and HO-1 in the human HepG2 cancer cell line.

The current work discovered that the PbAc-treated group's testicular tissue architecture displayed a variety of anomalies, including vacuolations. Some seminiferous tubules had an uneven shape, were filled with remnants of germinal epithelium, and were sloughed off the lamina propria. Wide interstitial tissue with dilated, congested blood vessels and eosinophilic exudate was seen. And these results agreed with (Albasher et al., 2021).

Darkly stained, apoptotic spermatogenic cell nuclei were visible in the tubules that were separated from the basal lamina and had discarded germinal epithelium. Additionally, broad, empty lumina and deformed tubules were seen. These were consistent with Johnson's explanation, which said that the fragmentation of the Sertoli cell which supplies the

spermatogenic cells with support and nourishment destroys testicular tissue and consequent infertility (Johnson, 2015).

A histological examination of rats given Pb showed that the germinal epithelium lining most of the seminiferous tubules was gradually degenerating. Similar findings have been reported by other researchers, who have characterized Pb-induced cell death as having a "washed-out" appearance (Celik et al., 2016).

The lead was documented to own the ability to cross the blood-testis barrier leading to separation of the basal lamina from Sertoli and germ cells in vitro (Awadalla et al., 2011). Lipid peroxidation, oxidative stress, and the generation of reactive oxygen species are the mechanisms through which the damage is caused. These processes can lead to the degeneration of spermatogenic cells and the disruption of the androgenic process by Leydig cells in the testis biological membranes (Wu et al., 2012).

In the PbAc+LUT-treated group, the H&E-stained sections showed marked improvement in the histological structure to be near the control group and these results were in harmony with the researchers who said that using LUT as a prophylactic step may be beneficial as it lessened the degree of the damage (Yahyazadeh and Altunkaynak, 2019; Al-Megrin et al., 2020).

The current histo-morphometric results, which exhibited a noteworthy decrease in the width and thickness of the germinal epithelium lining the seminiferous tubules in the PbAc-treated group compared to the control, confirmed these histological results. Alternatively, we found that the testes of the PbAc+LUT group had notably reduced damage. However, it is extremely noteworthy that LUT can reduce the effects of PbAc exposure.

Regarding Masson trichrome stained sections, there was a minimal distribution of collagen fibers in the capsule, basal lamina of seminiferous tubule, and wall of blood vessels of control and PbAc+LUT-treated groups and these results were agreed by (Melebary, 2022), their findings demonstrated that by enhancing the rats' antioxidant defenses. But shields homogenized rat testes from oxidative stress caused by Thioacetamide (TAA). but there was an excessive distribution of collagen fibers in the capsule, basal lamina of the seminiferous tubule, and wall of blood vessels in the PbAc-treated group and it was hypothesized by the inflammatory process in the testis, and subsequent disruption of the testicular morphology, leads to a change of the function of peritubular cells and increase in the fibrotic response (Mayerhofer, 2013).

Alpha-smooth muscle actin ( $\alpha$ -SMA) is a distinct marker for smooth muscle and myoepithelial cells and part of the cytoskeleton (Moustafa, 2012; Gabr et al., 2018). It impacts almost every bodily tissue, including the testicles, liver, heart, kidney, and pancreas (Ahmed, 2017). In this current study, there was a mild immune reaction for alpha-smooth muscle actin in the peritubular muscular coat in the control group, a mild reaction in PbAc+LUT-treated group, and a strong immune reaction for alpha-smooth muscle actin in the peritubular muscular coat and around blood vessels in PbAc treated group. Our results agreed with those of earlier studies (Nicolas et al., 2017; El-azab and Elmahalaway 2019), which showed a considerable rise in  $\alpha$ -SMA immunostaining with silver nanoparticles (AgNPs) over time. They also mentioned that the myoid cell proliferation and increased collagen fiber deposition thickened the lamina propria around degraded seminiferous tubules. Certain peritubular muscular coats (PMCs) underwent morphological alteration, becoming enlarged and asymmetrical in shape

with a profusion of cytoplasmic organelles, before evolving into myofibroblasts.

HSP70 is the family that includes glucose-regulated protein 78. This protein family's members are chaperones with ATP binding/hydrolysis capabilities, which facilitate their capacity to support protein folding, transport, and assembly by coordinating the protein substrate's sequential binding and release. At least seven distinct proteins make up the HSP70 family in mice, and multiple of them are essential for spermatogenesis (Georgopoulos and Welch., 1993).

In this current work, there was a higher cytoplasmic expression of GRP78 in the PbAc-treated group, moderate cytoplasmic expression of GRP78 in the PbAc+LUT-treated group, and a mild cytoplasmic expression of GRP78 in the control group and these findings were in accordance with (Wang et al., 2014).

It has been demonstrated that glucose-regulated protein 78 functions as a molecular chaperone and  $Ca^{2+}$  binding protein (Munro and Pelham, 1986). It is found in the endoplasmic reticulum and expressed in a variety of cell types (ER). Remarkably, GRP78 transcription is strongly stimulated in response to cellular stress. ER  $Ca^{2+}$  store depletion caused by tacsigargin (Tg) therapy, glucose starvation, and oxygen deprivation are all powerful inducers of GRP78 transcription. Thus, GRP78 can have a protective role in physiological settings in addition to its housekeeping roles like protein folding. Numerous investigations have revealed a link between somatic cells' resistance to apoptotic death and enhanced expression of GRP78, especially in tumors that are developing more rapidly (Reddy et al., 2003).

## Conclusion:

In summary, PbAc exposure caused lipid peroxidation and oxidative stress of testicular tissues through loss of internal antioxidant biomarkers like SOD and GPx, which concurrently increased the expression of genes that are sensitive to oxidative stress (Nrf2, Keap1, NQO1, and HO-1). Luteolin treatments protected rats' testicles from PbAc-persuaded oxidative stress by restoring internal antioxidants to normal levels and inhibiting Pb-persuaded testicular triggering of Nrf2/Keap1/NQO1/HO-1 signals.

**Conflict of interest:** This current work has no conflict of interest.

## References:

- Abdel Moneim, A. (2012).** 'Flaxseed oil as a neuroprotective agent on lead acetate-induced monoaminergic alterations and neurotoxicity in rats'. *Biol. Trace Elem. Res.*; 148(3)p.p.:363–370.  
<https://doi.org/10.1007/s12011-012-9370-4>
- Abdelhamid, F.M., Mahgoub, H.A., and Ateya, A.I. (2020).** 'Ameliorative effect of curcumin against lead acetate-induced hemato-biochemical alterations, hepatotoxicity, and testicular oxidative damage in rats'. *Environmental Science and Pollution Research International*, 27(10), pp. 10950–10965.
- Ahmed, R. (2017).** 'Histological assessment and quantification of hypervitaminosis A-induced fibrosis in liver, kidney and testis of albino rats'. *World J. Pharm. Sci.*, 5(8), pp. 209–220.
- Albarakati, A.J.A., Baty, R.S., Aljoudi, A.M., et al. (2020).** 'Luteolin protects against lead acetate-induced nephron-toxicity through antioxidant, anti-inflammatory, anti-apoptotic, and Nrf2/HO-1 signaling pathways'. *Molecular Biology Reports*, 47(4), pp. 2591–2603.
- Albasher, G., Alrajhi, R., Alshammry, E., et al. (2021).** 'Moringa oleifera leaf Extract attenuates Pb acetate-induced testicular damage in rats'. *Combinatorial Chemistry & High Throughput Screening*, 24(10), pp. 1593–1602.
- Al-Megrin, W.A., Alomar, S., Alkhuriji, A.F., et al. (2020).** 'Luteolin protects against testicular injury induced by lead acetate by activating the Nrf2/HO-1 pathway'. *IUBMB Life*, 72(8), pp. 1787–1798.
- Anyanwu, B.O., Ezejiyor, A.N., Igweze, Z.N., et al. (2018).** 'Heavy metal mixture exposure and effects in Developing Nations: An Update'. *Toxics*, 6(4), pp. 65.
- Aprioku J.S. (2013).** 'Pharmacology of free radicals and the impact of reactive oxygen species on the testis'. *Journal of Reproduction & Infertility*, 14(4), pp. 158–172.
- Awadalla, N.J., El-Helaly, M., Gouida, M., et al. (2011).** 'Sperm chromatin structure, semen quality and lead in blood and seminal fluid of Infertile Men'. *Int. J. of Occup. and Environ. Med.*, 2(1), pp. 27–36.
- Bancroft, J.D. and Gamble, M. (2008).** 'Theory and practice of histological techniques.' 6th Edition, Churchill Livingstone, Elsevier, China.
- Baty, R.S., Hassan, K.E., Alsharif, K.F., et al. (2020).** 'Neuroprotective role of luteolin against lead acetate-induced cortical damage in rats'. *Human and Experimental Toxicology*, 39(9), pp. 1200–1212.

- Celik, H., Camtosun, O., Ciftci, A., et al. (2016).** 'Beneficial effects of nerolidol on thioacetamide-induced damage of the reproductive system in male rats'. *Biomed. Res*, 27(3), pp. 725–730.
- Dyatlov, V.A., and Lawrence, D.A. (2002).** 'Neonatal lead exposure potentiates sickness behavior induced by *Listeria monocytogenes* infection of mice'. *Brain, Behavior, and Immunity*, 16(4), pp. 477–492.
- El-azab, N., and Elmahalaway, A. (2019).** 'A histological and immuno-histochemical study on testicular changes induced by silver nanoparticles in adult rats and the possible protective role of camel milk'. *Egyptian Journal of Histology*, 42(4): pp. 1044–1058.
- Elgawish, R.A.R., and Abdelrazek, H.M.A. (2014).** 'Effects of lead acetate on testicular function and caspase-3 expression with respect to the protective effect of cinnamon in albino rats'. *Toxicology Reports*, 1, pp. 795–801.
- Elmallah, M.I.Y., Elkhadragey, M.F., Al-Olayan, E.M., et al. (2017).** 'Protective effect of *Fragaria ananassa* crude extract on cadmium-induced lipid peroxidation, antioxidant enzymes suppression, and apoptosis in rat testes'. *International Journal of Molecular Sciences*, 18(5), pp. 957.
- El-Nekeety, A.A., El-Kady, A.A., Soliman, M.S., et al. (2009).** 'Protective effect of *Aquilegia vulgaris* (L.) against lead acetate -induced oxidative stress in rats'. *Food and Chemical Toxicology*, An International Journal Published for The British Industrial Biological Research Association, 47(9), pp. 2209–2215.
- Gabr, S., Zahran, F., Mohammed, F., et al. (2018).** 'Therapeutic effect of camel milk against hepatotoxicity induced by CCL4 in rats'. *Research Journal of Pharmaceutical, Biological and Chemical Sciences*, 9(1), pp. 601–614.
- Georgopoulos, C., and Welch, W.J. (1993).** 'Role of the major heat shock proteins as molecular chaperones'. *Annual Review of Cell Biology*, 9, pp. 601–634.
- Hamdan, M., Noorhamdani, A.S., Rahayu, M. et al. (2020).** 'The effect of Ginkgo Biloba (Egb) extracts on the expression of Hsp 90, Vegf and Bdnf in the *Rattus Novergicus* with lead (Pb) exposure'. *J. Int. Dent. Med. Res.*, 13(1), pp. 17–22.
- Ijaz, M., Ayaz, F., Mustafa, S., et al. (2022).** 'Toxic effect of polyethylene microplastic on testicles and ameliorative effect of luteolin in adult rats: Environmental challenge'. *Journal of King Saud University - Science*, 34(4), pp. 102064.
- Ijaz, M.U., Haider, S., Tahir, A., et al. (2023).** 'Mechanistic insight into the protective effects of fisetin against arsenic-induced reproductive toxicity in male rats'. *Scientific Reports*, 13(1), pp. 3080.
- Johnson K.J. (2015).** 'Testicular histopathology associated with disruption of the Sertoli cell cytoskeleton'. *Spermatogenesis*, 4(2), pp. e979106.
- Kalbolandi, S.M., Gorji, A.V., Babaahmadi-Rezaei, H., et al. (2019).** 'Luteolin confers renoprotection against ischemia -reperfusion injury via involving Nrf2 pathway and regulating miR320'. *Molecular Biology Reports*, 46(4), pp. 4039–4047.
- Kelainy, E.G., Ibrahim Laila, I.M., and Ibrahim, S.R. (2019).** 'The effect of ferulic acid against lead-induced oxidative stress and DNA damage in kidney and testes of rats'. *Environmental*

*Science and Pollution Research International*, 26(31), pp. 31675–31684.

- Kempuraj, D., Thangavel, R., Kempuraj, D.D., et al. (2021).** 'Neuroprotective effects of flavone luteolin in neuro-inflammation and neuro-trauma'. *BioFactors (Oxford, England)*, 47(2), pp. 190–197.
- Li, L., Dong, H., Song, E., et al. (2014).** 'Nrf2/ARE pathway activation, HO-1 and NQO1 induction by polychlorinated biphenyl quinone is associated with reactive oxygen species and PI3K/AKT signaling'. *Chemico - Biological Interactions*, 209, pp. 56–67.
- Livak, K.J., and Schmittgen, T.D. (2001).** 'Analysis of relative gene expression data using real-time quantitative PCR and the 2(-Delta Delta C(T)) Method'. *Methods (San Diego, Calif.)*, 25(4), pp. 402–408.
- Mabrouk, A. and Ben Cheikh, H. (2016).** 'Thymoquinone supplementation ameliorates lead -induced testis function impairment in adult rats'. *Toxicology and Industrial Health*, 32(6), pp. 1114–1121.
- Marklund, S., and Marklund, G. (1974).** 'Involvement of the superoxide anion radical in the autoxidation of pyrogallol and a convenient assay for superoxide dismutase'. *European Journal of Biochemistry*, 47(3), pp. 469–474.
- Massányi, P., Massányi, M., Madeddu, R., et al. (2020).** 'Effects of cadmium, lead, and mercury on the structure and function of reproductive organs'. *Toxics*, 8(4), pp. 94.
- Mayerhofer, A. (2013).** 'Human testicular peritubular cells: more than meets the eye'. *Reproduction (Cambridge, England)*, 145(5), pp. R107–R116.
- Melebary, S. (2022).** 'The possible protective effect of luteolin in a thioacetamide rat model of testicular toxicity'. *Int. J. Agric. Biol.*, 28(6), pp. 391–404.
- Moustafa, A. (2012).** 'Age-related changes in the immunohistochemical localization pattern of  $\alpha$ -smooth muscle actin and vimentin in rat testis'. *The Egyptian Journal of Histology*, 35(3), pp. 412–423.
- Munro, S., and Pelham, H.R. (1986).** 'An Hsp70-like protein in the ER: identity with the 78 kd glucose-regulated protein and immunoglobulin heavy chain binding protein'. *Cell*, 46(2), pp. 291–300.
- Nicolas, N., Michel, V., Bhushan, S., et al. (2017).** 'Testicular activin and follistatin levels are elevated during the course of experimental autoimmune epididymo-orchitis in mice'. *Scientific Reports*, 7, pp. 42391.
- Ohkawa, H., Ohishi, N., and Yagi, K. (1979).** 'Assay for lipid peroxides in animal tissues by thiobarbituric acid reaction'. *Analytical Biochemistry*, 95(2), pp. 351–358.
- Owumi, S.E., Ijadele, A.O., Okuu, A.U., et al. (2020).** 'Luteolin abates reproductive toxicity mediated by the oxido-inflammatory response in Doxorubicin-treated rats'. *Toxicology Research and Application*, 4, pp.1–16.
- Paglia, D.E., and Valentine, W.N. (1967).** 'Studies on the quantitative and qualitative characterization of erythrocyte glutathione peroxidase'. *The Journal of Laboratory and Clinical Medicine*, 70(1), pp. 158–169.
- Rakoczy, K., Kaczor, J., Soltyk, A., et al. (2023).** 'Application of luteolin in neoplasms and nonneoplastic diseases'. *Int. J. Mol. Sci.*, 24(21), pp. 15995.

- Reddy, R.K., Mao, C., Baumeister, P., et al. (2003).** 'Endoplasmic reticulum chaperone protein GRP78 protects cells from apoptosis induced by topoisomerase inhibitors: role of ATP binding site in suppression of caspase-7 activation'. *The Journal of Biological Chemistry*, 278(23), pp. 20915–20924.
- Ross, D., and Siegel, D. (2017).** 'Functions of NQO1 in cellular protection and CoQ<sub>10</sub> metabolism and its potential role as a Redox sensitive molecular switch'. *Frontiers in Physiology*, 8, pp. 595.
- Somade, O.T., Adeyi, O.E., Ajayi, B.O., et al. (2022).** 'Syringic and ascorbic acids prevent NDMA-induced pulmonary fibrogenesis, inflammation, apoptosis, and oxidative stress through the regulation of PI3K-Akt/PKB-mTOR-PTEN signaling pathway'. *Metabolism Open*, 14, pp. 100179.
- Sudjarwo, S.A., Sudjarwo, G.W., and Koerniasari (2017).** 'Protective effect of curcumin on lead acetate-induced testicular toxicity in Wistar rats'. *Research in Pharmaceutical Sciences*, 12(5), pp. 381–390.
- Taheri, Y., Sharifi-Rad, J., Antika, G., et al. (2021).** 'Paving luteolin therapeutic potentialities and agro-food-pharma applications: Emphasis on *In vivo* pharmacological effects and bioavailability traits'. *Oxid. Med. Cell Longev.*, 2021, pp. 1987588.
- Teerasarntipan, T., Chaiteerakij, R., Prueksapanich, P., et al. (2020).** 'Changes in inflammatory cytokines, antioxidants and liver stiffness after chelation therapy in individuals with chronic lead poisoning'. *BMC Gastroenterology*, 20(1), pp. 263.
- Udefa, A.L., Amama, E.A., Archibong, E.A., et al. (2020).** 'Antioxidant, anti-inflammatory and anti-apoptotic effects of hydro-ethanolic extract of *Cyperus esculentus* L. (tigernut) on lead acetate-induced testicular dysfunction in Wistar rats'. *Biomedicine and Pharmacotherapy*, 129, pp. 110491.
- Ulasov, A.V., Rosenkranz, A.A., Georgiev, G.P., et al. (2022).** 'Nrf2/Keap1/ARE signaling: towards specific regulation'. *Life Sciences*, 291, pp. 120111.
- Wahab, O.A., Princely, A.C., Oluwadamilare, A.A., et al. (2019).** 'Clomiphene citrate ameliorated lead acetate-induced reproductive toxicity in male Wistar rats'. *JBRA Assisted Reproduction*, 23(4), pp. 336–343.
- Wang, W., Wang, X., Zhu, P., et al. (2014).** 'Expression and location of glucose-regulated protein 78 in testis and epididymis'. *West Indian Medical Journal*, 1(1), pp. 14–17.
- Wu, H.M., Lin-Tan, D.T., Wang, M.L., et al. (2012).** 'Lead level in seminal plasma may affect semen quality for men without occupational exposure to lead'. *Reproductive Biology and Endocrinology*, 10(91), PMC3520831.
- Yahyazadeh, A., and Altunkaynak, B.Z. (2019).** 'Protective effects of luteolin on rat testis following exposure to 900 MHz electromagnetic field'. *Biotechnic & Histochemistry: Official Publication of the Biological Stain Commission*, 94(4), pp. 298–307.